Diffusion doping route to plasmonic Si/SiO_x nanoparticles

S.S. Bubenov [a], S.G. Dorofeev [a], A.A. Eliseev [a,b], N.N. Kononov [c], A.V. Garshev [b], N.E. Mordvinova [a,d], O.I. Lebedev [d]

[a] Department of Chemistry, Lomonosov Moscow State University, 1-3 Leninskie Gory, Moscow 119991, Russia
[b] Department of Materials Science, Lomonosov Moscow State University, 1-73 Leninskie Gory, Moscow 119991, Russia
[c] Prokhorov General Physics Institute, Russian Academy of Sciences, 38 Vavilova st., Moscow 119333, Russia
[d] Laboratoire CRISMAT, UMR6508, CNRS-ENSICAEN, 6 boulevard Marechal Juin, Caen 14050, France

Electronic Supplementary Information

I. Results of thermopower measurements.

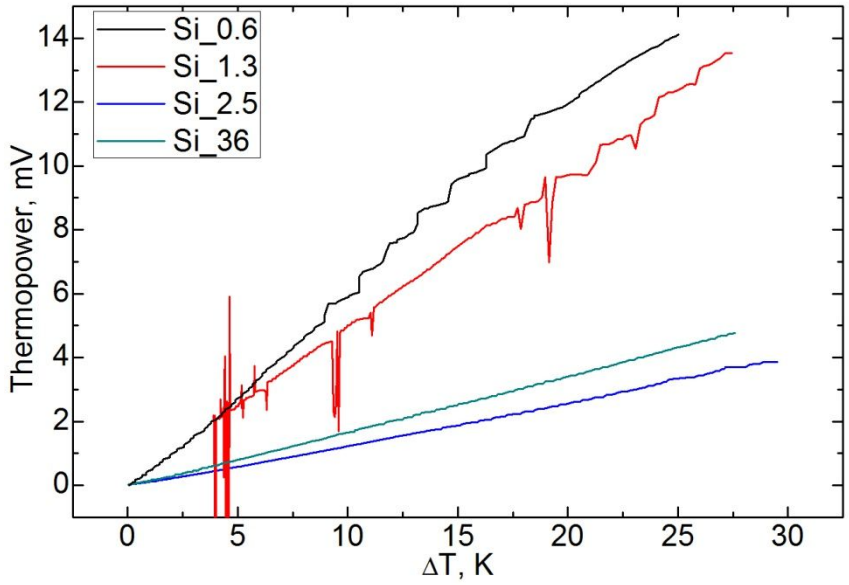

Figure S1. Thermopower generated by pellet samples of doped semiconductor nanoparticles vs temperature difference between top and bottom contacts; temperature of massive bottom contact was 23°C (see main text).

II. General characterization of IR spectra of the samples.

Examination of IR spectra of synthesized samples of silicon semiconductor nanoparticles (SNPs) in wavenumber region >700 cm^{-1} reveals the following. Every sample both in KBr pellet and in thin film form exhibits a peak at ~1060 cm^{-1} with two prominent shoulders at 870 and 1200 cm^{-1} and a broad band spanning over 3000-3700 cm^{-1}. The former feature is accounted for with $\delta_{H\text{-}Si\text{-}O3}$ (870 cm^{-1}), $\nu_{Si\text{-}O\text{-}Si,\ TO}$ (1100 cm^{-1}) and $\nu_{Si\text{-}O\text{-}Si,\ LO}$ (1200 cm^{-1}) modes [s1,s2], while the latter is due to $\nu_{Si\text{-}OH}$ (3200-3700 cm^{-1}) [s2] and ν_{OH} of water and other hydroxyl groups. Some spectra also show two peaks at ~1400 and ~1600 cm^{-1}. These correspond to deformational ν_α modes of OH^- and H_2O, respectively [s3]. $\nu_{Si\text{-}O\text{-}Si}$ and ν_α features are situated in a spectral region of prominent absorption of localized surface plasmon resonance (LSPR) band when the latter is present in the spectrum. As a consequence of considerable coupling ν_α vibrations are then very asymmetrical and $\nu_{Si\text{-}O\text{-}Si}$ appear to have asymmetric "Fano-type" profile against the background of LSPR. The LSPR band in the studied samples has a maximum in 1600-2200 cm^{-1} region and a considerable FWHM of ~2000 cm^{-1}. Characteristic triple feature of methyl and methylene groups is also observed in some samples: $\nu_{s,\ C\text{-}H,\ methylene}$ (2860 cm^{-1}), $\nu_{as,\ C\text{-}H,\ methylene}$ (2930 cm^{-1}), $\nu_{s,\ C\text{-}H,\ methyl}$ (2960 cm^{-1}). $\nu_{as,\ C\text{-}H,\ methyl}$ mode is also present, as indicated by increased absorption at ~2880 cm^{-1}. The methyl and methylene features are mainly present in etched samples, as hydride terminated nanosilicon is a strong reducing agent and is capable of reducing CO_2 from atmosphere or, possibly, traces of ethanol in sols of SNPs. Spectral peculiarities of individual samples are summarized in Table S1.

Table S1. Presence, intensity and position of select bands in IR spectra of samples of Si SNPs.

Sample	Acquisition regime: form of sample/ preconditioning		number of etching steps	LSPR mode position, cm^{-1}	ν_{α}	$\nu_{s,\ C\text{-}H,}$ and $\nu_{as,\ C\text{-}H}$	$\nu_{Si\text{-}OH}$ and ν_{OH}
Si_0	pellet		0	none	+		prominent
	film		-//-	-//-	+	+	prominent
		degassed	-//-	-//-		+	minor
Si_1.3	pellet		-//-	-//-	+	+	prominent
	film		-//-	-//-	+	+	prominent
		degassed	-//-	-//-	+		minor
Si_2.5	pellet		-//-	-//-	+	+	prominent
Si_9.1	film		-//-	1860			prominent
			1	1800	+	+	-//-
			2	~1800	+	+	-//-
		degassed	0	1990			minor
			1	2030	+	+	-//-
			2	2190	+	+	-//-
Si_20	pellet		0	1760	+	+	prominent
	film		0	1880			-//-
			1	1913	+	+	-//-
			2	1790	+	+	-//-
		degassed	0	1990			minor
			1	2030		+	-//-
			2	1880		+	-//-
Si_36	pellet		0	1890	+	+	prominent
	film		0	1710			-//-
			1	1850	+	+	-//-
			2	1830	+	+	-//-
			3	~1660	+	+	-//-
			4	~1600	+	+	-//-
		degassed	0	1840			minor
			1	2050			-//-
			2	2020			-//-
			3	1990		+	-//-
			4	1800			-//-

III. Lattice expansion evaluation with thermal dependence of XRD pattern.

Thermal XRD experiment was performed for the sample Si_20. As broad amorphous halo is present at 2θ of ~22°, diffraction angle region 15 - 26° was excluded from fits. Additional peaks appeared upon heating to 550°C, that are artifacts associated with material redeposition in the high-temperature attachment (peaks at 2θ ≈ 37.7; 43,8°. Ag: ICDD number 4-783), so regions of 36 - 39°, 42.5 - 45° were omitted as well for that measurement. Lorentian profile allowed to adequately fit diffraction peaks and lattice parameter was determined for different temperatures (Fig.S2).

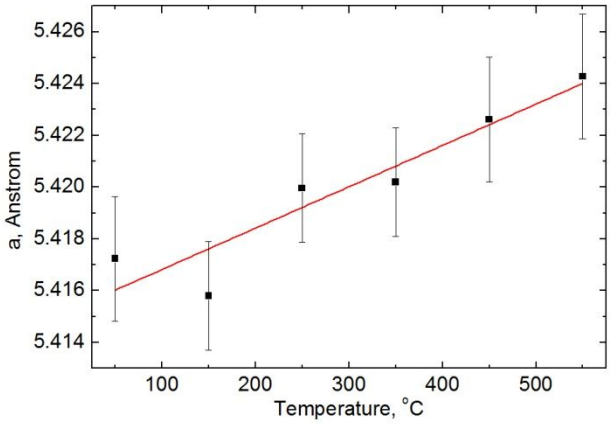

Figure S2. Lattice parameter of Si cores in sample Si_20 at different temperatures and linear fit of the data.

As a result, linear expansion coefficient α_L can be estimated as $3.0\pm1.5\cdot10^{-6}$ K^{-1}. Corresponding changes in the position of plasmonic peak ω_{sp} can derived by the following:

$$\frac{\Delta\omega_{SP}}{\omega_{SP}} = \left(1+\frac{\Delta N_c}{N_c}\right)^{1/2} - 1 = \left(\frac{1}{1+\Delta V/V}\right)^{1/2} - 1 = (1+\alpha_L\cdot\Delta T)^{-3/2} - 1 \approx -\frac{3}{2}\alpha_L\Delta T; \quad (S1)$$

where N_C is the free carrier concentration, V - the unit cell volume, T - the temperature. Thus, one can estimate the effect of heating on the position of the maximum as 0.1 - 0.3% (ΔT = 420 K). The sample under consideration exhibited 4% reversible loss in ω_{sp} when heated from 30 to 450°C. The value of the same effect for other samples is in the range of 1.7-18%. Thus, thermal expansion of lattice does not account for the red shift of plasmonic peak upon heating, observed for P-doped Si SNPs.

IV. Fitting of localized surface plasmon resonance band of P-doped Si nanoparticles

Plasmonic properties of dispersions and films of SNPs are frequently described with a combination of dielectric response of metallic media given by Drude theory and absorption of microspheres according to Mie theory [s1,s4].

Dielectric function of SNPs ε_P is then given by:

$$\varepsilon_p = \varepsilon_\infty - \frac{\omega_p^2}{\omega^2 + i\omega\Gamma}; \text{ (S2)}$$

where ω is the excitation frequency, ε_∞ - the high-frequency dielectric constant of SNPs, ω_p - the plasmonic frequency of SNPs, Γ - the damping term, i - the imaginary unit.

Absorbance A of core/shell microspheres in quasistatic limit given by Mie theory [s4] is:

$$A(\omega) = \beta \varepsilon_M^{0.5} \omega \cdot \mathrm{Im}\left(\frac{(\varepsilon_S - \varepsilon_M)(\varepsilon_P(\omega) + 2\varepsilon_S) + \alpha(\varepsilon_P(\omega) - \varepsilon_S)(\varepsilon_M + 2\varepsilon_S)}{(\varepsilon_S + 2\varepsilon_M)(\varepsilon_P(\omega) + 2\varepsilon_S) + 2\alpha(\varepsilon_P(\omega) - \varepsilon_S)(\varepsilon_S - \varepsilon_M)}\right); \text{ (S3)}$$

where ε_M - the dielectric constant of surrounding medium, α is the volume ratio of cores to the whole nanoparticles, ε_S is the dielectric constant of the shell, β is the prefactor given by the following expression:

$$\beta = \frac{6\pi L f_V}{c \cdot \ln(10)}; \text{ (S4)}$$

where f_V is the volume fraction of SNPs in the sample, L - the optical path length, c - the speed of light.

Spectral region with wavenumber above 1380 cm^{-1} was considered for fitting, as below that SiO_x absorption is significant. The following constants were adopted ε_∞ = 10.28 [s5], ε_M = 1, α = 0.579. The latter value was obtained with results of EDX elemental mapping and XRD discussed in the main body of the article, as well as with elemental analysis of undoped SNPs, revealing mass fraction of silicon of 77%. ε_S was treated as real and was modeled by (2.105 - 131.3·exp(-ω[cm^{-1}]/285.6) [s6,s7]. Scattering was accounted for with $c1 + c2 \cdot \omega^4$ baseline [s8].

ω_p, Γ, β, $c1$, $c2$ were fit parameters. The fit curves deviate the experimental spectra considerably (Fig. S3), so modifications to the model were sought for.

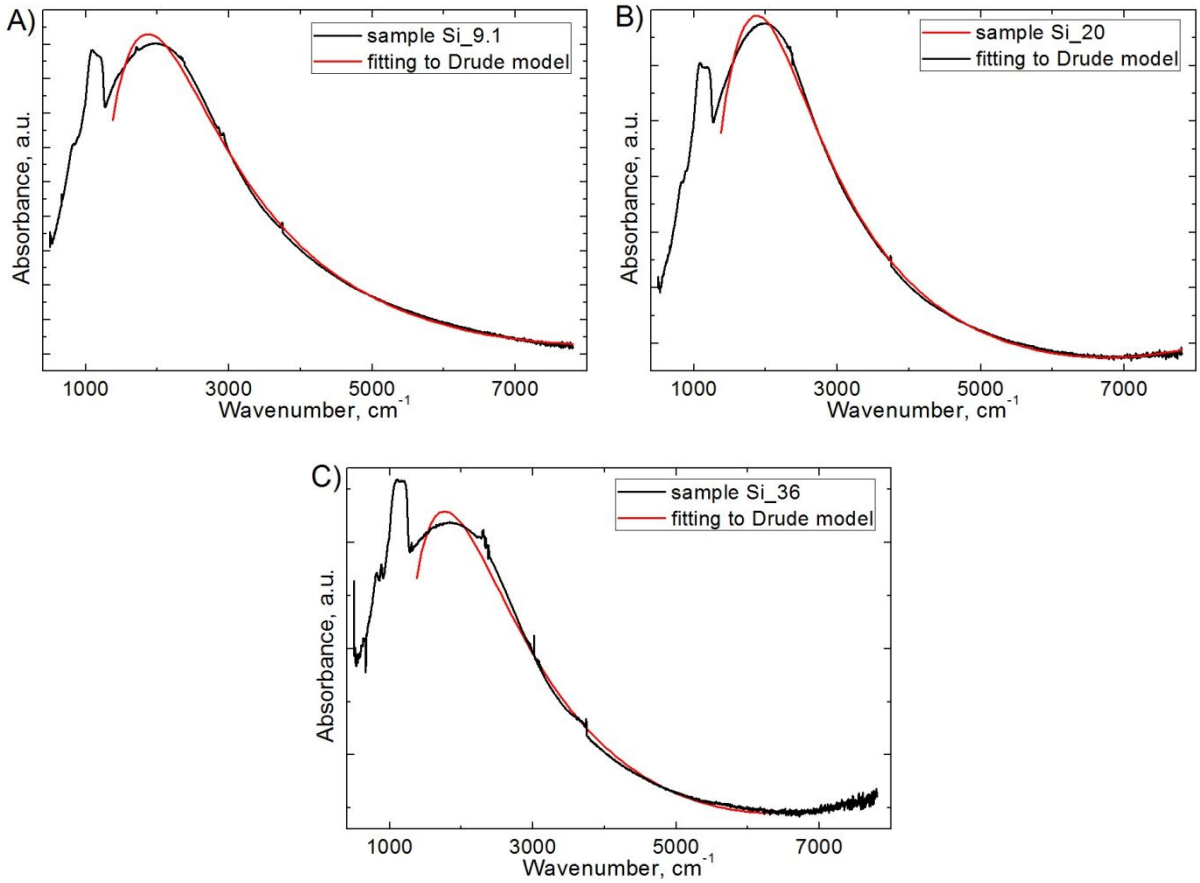

Figure S3. Fitting of IR spectra of Si nanoparticles to Drude oscillator - Mie theory absorption model: A) sample Si_9.1; B) sample Si_20; C) sample Si_36.

Firstly, applicability of Eq.S3 was considered. It is only valid for absorption of plasmonic microspheres up to f_v values of ~0.01, while f_v of Si cores in drop-cast films used in this work is about 0.1. An alternative quantification in form of the effective medium approximation accounts for far-field interactions in less dilute dispersions and predicts rather minute deviations from Eq.S3 in the form of the spectrum for $f_v < 0.2$ especially for the lower wavelength slope of the peak [s4].

Moreover, spectra of SNPs registered for thin films and for pressed KBr pellets exhibit similar lineshapes (Fig.S4). In the latter regime f_v is $\sim 5 \cdot 10^{-4}$ and Eq.S3 should be applicable. In that regard, further enhancements to the model were sought in modification of Eq.S2.

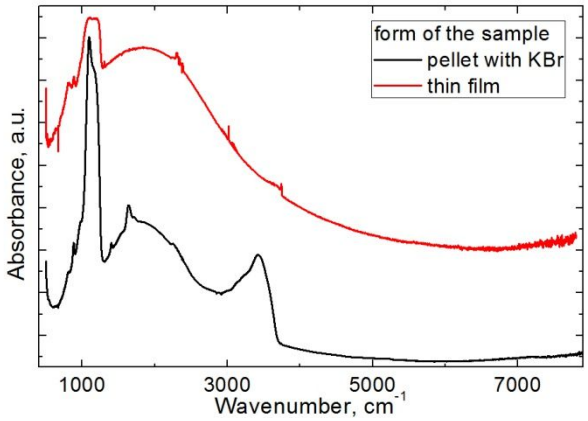

Figure S4. IR spectra of Si_36 sample both in form of pressed pellet with KBr and in form of thin film (see main text). The spectra are offset vertically for clarity.

Indeed, the use of single ω_p and Γ values for an ensemble of SNPs is a simplified approach. Ensemble variation of ω_p results in smearing of the peak, perceived as increased FWHM. The absorption spectra of such compositionally inhomogeneous samples are still fit reasonably well with use of Eq.S2, resulting only in a slight error in obtained mean ω_p, while damping term Γ is greatly overestimated [s4]. On the other hand, nanoparticle size induced variation of Γ counterintuitively leads to slight sharpening of the peak [s4], that isn't observed in case of samples of doped SNPs under consideration. Moreover, both of these phenomena do not account for $\sim\lambda^{1.5}$ dependence of lower wavelength slope of the peak, discussed in the main body of the article.

Finally, a model with frequency-dependent damping term was considered to account for the power law of the slope and for temperature dependence of the spectra. The following expression was used [s4]:

$$\Gamma = \frac{\Gamma_H \omega^4 + \Gamma_L \omega_0^4}{\omega^4 + \omega_0^4}; \text{ (S5)}$$

where Γ_L is the low-frequency damping constant, Γ_H - the high-frequency one, ω_0 - the cross-over frequency. IR spectra of a sample at different temperatures were fit simultaneously to resolve overparameterization, parameters β, ω_p, Γ_H were considered temperature independent and were shared during the fitting. Resultant fits and Γ(ω) dependences are shown in Fig. S5.

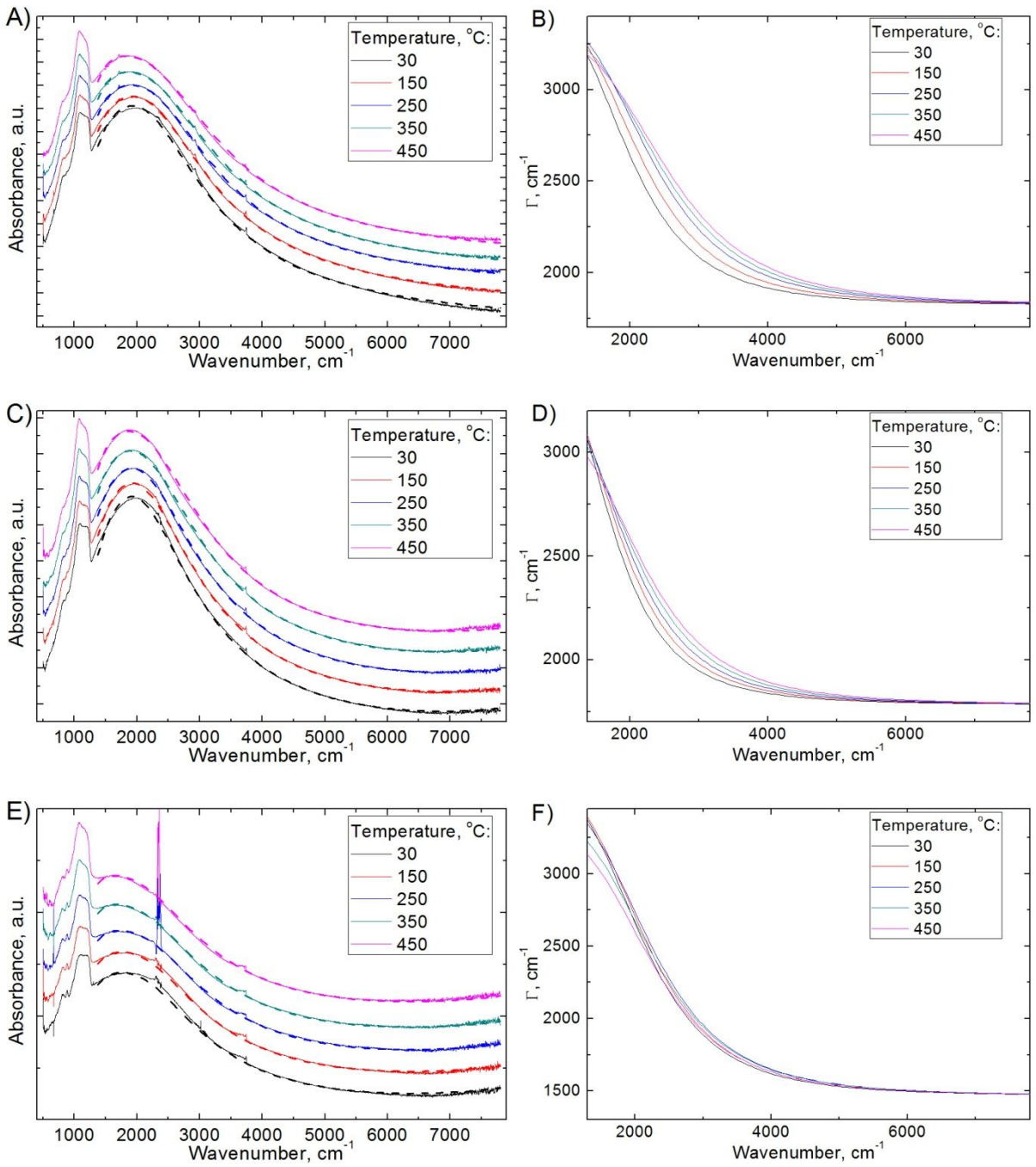

Figure S5. Results of fitting of IR spectra of plasmonic samples at different temperatures: A,C,E) IR spectra (solid lines) and fit curves (dashed lines) for samples Si_9.1, Si_20, Si_36, the spectra are offset vertically for clarity; B,D,F) spectral dependences of the damping term for samples Si_9.1, Si_20, Si_36, respectively.

Plasmonic frequencies corresponding to different fits are summarized in Table S2. A simplistic evaluation by:

$$\omega_P = \omega_{SP} \cdot \sqrt{\varepsilon_\infty + 2\varepsilon_M}; \text{ (S6)}$$

is also given. Results of fitting that assumed frequency dependent damping were used for evaluation of carrier generation efficiency.

Table S2. Plasmonic frequencies of samples Si_9.1, Si_20, Si_36, calculated with different approaches. Results used for calculation of carrier generation efficiency are in bold.

Sample	Plasmonic frequency, cm^{-1}		
	Fitting (ω-independent damping term)	Fitting (ω-dependent damping term)	Eq.S6
Si_9.1	6600	**5500**	7000
Si_20	6700	**5600**	7000
Si_36	6200	**3700**	6400
Si_9.1 etched	6600	**5700**	7100
Si_20 etched	7500	**7400**	7200
Si_36 etched	7100	**6700**	7200

References:

s1. Zhou, S.; Pi, X.; Ni, Z.; Ding, Y.; Jiang, Y.; Jin, C.; Delerue, C.; Yang, D.; Nozaki, T. Comparative Study on the Localized Surface Plasmon Resonance of Boron- and Phosphorus-Doped Silicon Nanocrystals *ACS Nano* **2015**, 9, 378.

s2. Stuart, B. Infrared spectroscopy: fundamentals and applications; John Wiley & Sons, 2004.

s3.Yukhnevich, G. V. Infrared spectroscopy of water; Nauka: Moscow, 1973.

s4. Mendelsberg, R. J.; Garcia, G.; Li, H.; Manna, L.; Milliron, D. J. Understanding the Plasmon Resonance in Ensembles of Degenerately Doped Semiconductor Nanocrystals *J. Phys. Chem. C* **2012**, 116, 12226.

s5. Lannoo, M.; Delerue, C.; Allan, G. Screening in Semiconductor Nanocrystallites and Its Consequences for Porous Silicon *Phys. Rev. Lett.* **1995**, 74, 3415.

s6. Grigor'ev, I. S.; Mejlihov, E. Z. *Physical values*; Energoatomizdat: Moscow, 1991.

s7. Efimov, A. M.; *Optical Constants of Inorganic Glasses*; CRC Press: Boca Raton, FL, 1995.

s8. Bohren, C. F.; Huffman, D. R. *Absorption and Scattering of Light by Small Particles*; Wiley-VCH: Weinheim, 2004.